DOI: 10.1002/cmdc.201200582

Benzenesulfonamides: A Unique Class of Chemokine Receptor Type 4 Inhibitors

Suazette Reid Mooring,*[a, b] Jin Liu,[c] Zhongxing Liang,[a, d] Jeffrey Ahn,[a] Samuel Hong,[a] Younghyoun Yoon,[a] James P. Snyder,*[c] and Hyunsuk Shim*[a, d]

The interaction of CXCR4 with CXCL12 (SDF-1) plays a critical role in cancer metastasis by facilitating the homing of tumor cells to metastatic sites. Based on our previously published work on CXCR4 antagonists, we have synthesized a series of aryl sulfonamides that inhibit the CXCR4/CXCL12 interaction. Analogue bioactivities were assessed with binding affinity and Matrigel invasion assays. Computer modeling was employed to evaluate a selection of the new analogues docked into the CXCR4 X-ray structure and to rationalize discrepancies between the affinity and Matrigel in vitro assays. A lead compound displays nanomolar potency in the binding affinity assay (IC_{50} = 8.0 nM) and the Matrigel invasion assay (100% blockade of invasion at 10 nM). These data demonstrate that benzenesulfonamides are a unique class of CXCR4 inhibitors with high potency.

Introduction

The G-protein-coupled receptor (GPCR) CXCR4 and the chemokine stromal cell-derived factor-1 (SDF-1, also known as CXCL12) play a crucial role in physiological processes such as leukocyte migration/trafficking and hematopoiesis.[1] The interaction of CXCL12 with CXCR4 has implications in cancer metastasis,[2] and CXCR4 is a co-receptor for HIV-1 infection.[3] CXCR4 is frequently overexpressed in solid tumors as compared with normal tissue.[4] Activation of the CXCR4/CXCL12 pathway can lead to the recruitment of distal stroma by tumor cells to facilitate tumor growth and metastasis, and can promote homing of tumor cells to metastatic sites,[5] angiogenesis,[6] cancer cell survival, and invasion.[4,7] Therefore, disruption of the interaction between CXCL12 and CXCR4 could block or delay metastasis.

Thus far, the most explored non-peptidic anti-CXCR4 agents are bicyclams such as AMD3100 and its derivatives.[8] However, their metal-chelating properties may be the cause of cardiotoxicity and therefore may well limit the clinical use of these compounds.[8] We recently identified a novel class of CXCR4 antagonists[9] that led to a potent dipyridine: WZ811 (**1**; Figure 1). Potent pyridine and dipyrimidine analogues have been synthesized by our research group[10] and by others.[11] Exploration of tunable areas around the dipyridine pharmacophore led us to prepare a new class of benzenesulfonamide analogues (Figure 2). The central phenyl ring was retained because it has been shown to be important for inhibitory activity.[9a] A binding affinity assay against the potent CXCR4 antagonist TN14003 (**2**; Figure 1) was employed as a primary screening method for the new analogues.[9a,12] Some of these compounds were further

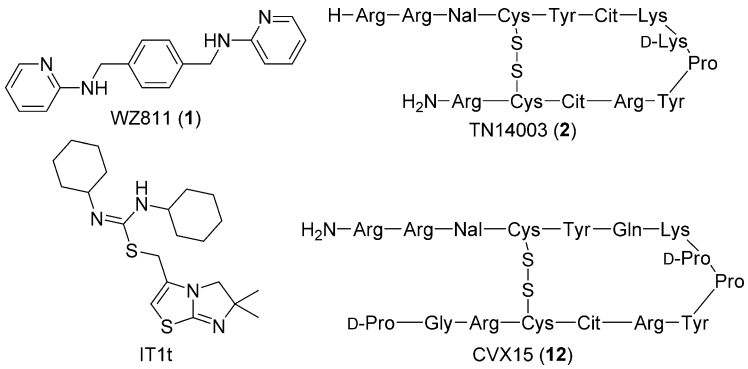

Figure 1. Structures of CXCR4 blockers IT1t, **1**, and peptidic antagonists **2** and **12**.

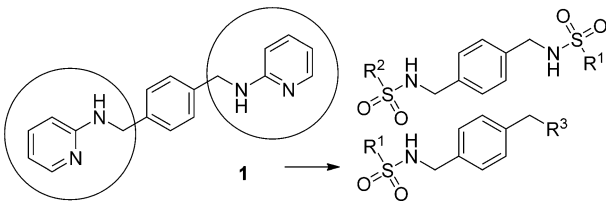

Figure 2. Design of new sulfonamide analogues based on the scaffold of compound **1** (R^1, R^2, and R^3: alkyl or aryl substituents).

[a] Dr. S. R. Mooring, Dr. Z. Liang, J. Ahn, S. Hong, Dr. Y. Yoon, Dr. H. Shim
Department of Radiology and Imaging Sciences
Emory University, Atlanta, GA (USA)
E-mail: hshim@emory.edu

[b] Dr. S. R. Mooring
Current address: Department of Chemistry
Georgia State University, Atlanta, GA (USA)
E-mail: smooring@gsu.edu

[c] Dr. J. Liu, Dr. J. P. Snyder
Department of Chemistry and Emory Institute for Drug Discovery
Emory University, Atlanta, GA (USA)
E-mail: jsnyder@emory.edu

[d] Dr. Z. Liang, Dr. H. Shim
Winship Cancer Institute, Emory University, Atlanta, GA (USA)

analyzed in the Matrigel invasion assay by using full-length CXCL12.

Chemistry

A small series of mono- and disulfonamide analogues of **1** (Figure 2) were prepared with a selection of substituents to test the viability of this structural class as CXCR4 antagonists. Compounds **3a** and **3b** were synthesized in one step by the reaction of xylylenediamine with the corresponding sulfonyl chlorides (Scheme 1). Compounds **5a**–**n** were prepared by the treatment of 4-(bromomethyl)benzenesulfonyl chloride with the corresponding secondary amine to give compounds **4a**–**d**, which were treated with the appropriate amine to give the final products (Scheme 2). Compound **7** was obtained similarly by treating 4-(bromomethyl)benzenesulfonyl chloride with *N*-methyl-2-pyridinemethanamine to give **6**, which was subsequently coupled with pyrrolidine in the presence of potassium carbonate to give the final target (Scheme 2). As shown in Scheme 3, *N*-Boc-4-hydroxyaniline was treated with 2-chloro-*N*,*N*-diethylethanamine to yield **8** and subsequently deprotected with hydrochloric acid in dioxane to give **9** as the hydrochloride salt. Compound **9** was then combined with 4-(bromomethyl)benzenesulfonyl chloride to give **10**, which yielded **11a**–**d** upon treatment with the corresponding amines.

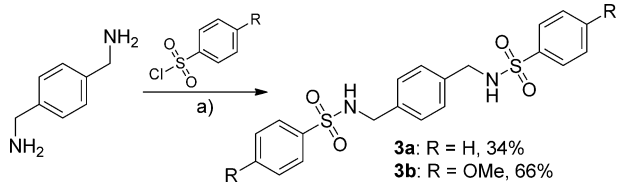

Scheme 1. Synthesis of **3a** and **3b**. *Reagents and conditions*: a) DIPEA, CH_2Cl_2, RT, 3 h.

Results and Discussion

Binding affinity assays

The compounds were initially screened with a binding affinity assay involving competition of **2** with the putative antagonists, as described in our previous publications.[12,9a] MDA-MB-231 cells were pre-incubated with compounds at concentrations of 1, 10, 100, and 1000 nM, then incubated with biotinylated **2** and streptavidin-conjugated rhodamine to determine the binding efficiency of the new analogues to the CXCL12 binding domain of CXCR4. The effective concentration (EC) is defined as the lowest concentration at which a significant decrease in rhodamine fluorescence is observed relative to control, reflecting competitive displacement by **2**. Therefore, this screen is a semi-quantitative first-pass measure of the level of activity, and should not be confused with IC_{50} determination.

Initially, five compounds—**3a**, **3b**, **5a**, **5b**, and **11a**—were synthesized and analyzed for binding. As shown in Table 1, the disulfonamides **3a** and **3b** were found to be relatively inactive. However, the monosubstituted sulfonamides **5a**, **5b**, and **11a** were more effective, with respective EC values of 10, 1, and 10 nM. Hence, we pursued analogues with the monosubstitut-

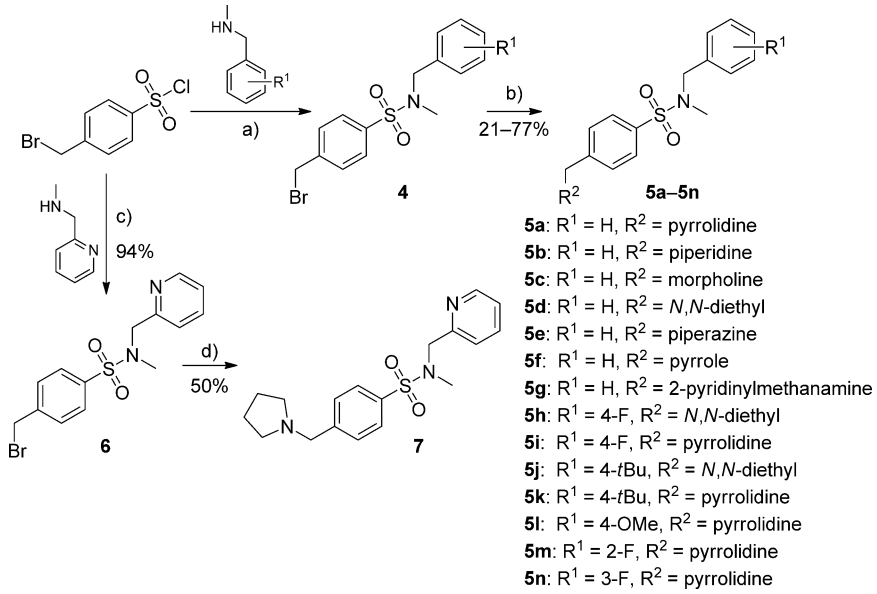

Scheme 2. Synthesis of **5a**–**n** and **7**. *Reagents and conditions*: a) CH_2Cl_2, RT, 12 h; b) amine, Et_3N or K_2CO_3, CH_2Cl_2 or CH_3CN, RT, 12 h; c) CH_2Cl_2, RT, 12 h; d) pyrrolidine, K_2CO_3, CH_3CN, RT, 12 h.

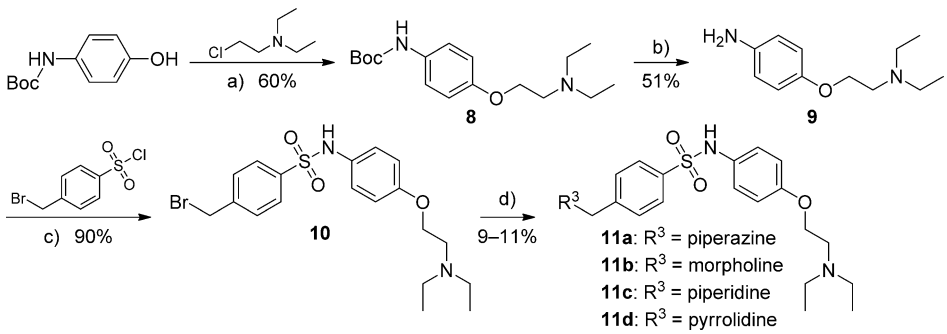

Scheme 3. Synthesis of **11a**–**d**. *Reagents and conditions*: a) CH_2Cl_2, RT, 3 h; b) HCl/dioxane, dioxane, RT, 12 h; c) DIPEA, THF/DMF, RT, 12 h; d) amine, CH_2Cl_2, RT, 12 h.

Table 1. Sulfonamide analogues **3** and **5** evaluated by binding affinity and Matrigel invasion assays.

Compound		EC [nM]	Invasion inhib. [%][a] 10 nM	100 nM
3a	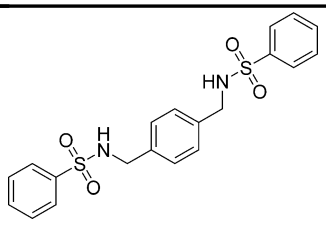	1000	NA	NA
3b	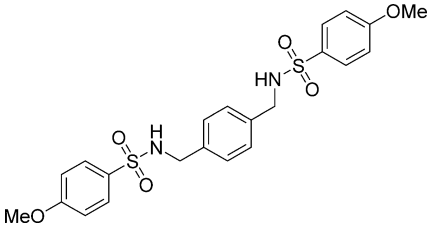	1000	95	100
5a	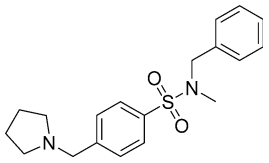	10	100	100
5b	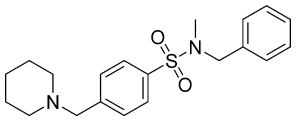	1	94	100
5c	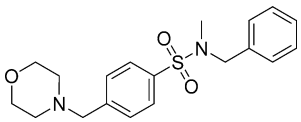	1000	0	76
5d	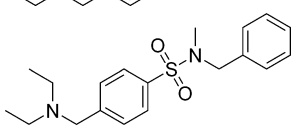	10	71	84
5e	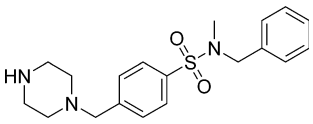	1	78	76
5f	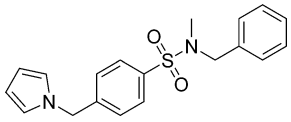	>1000	32	61
5g	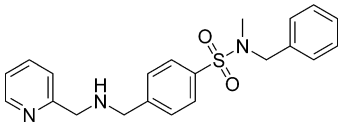	100	48	72
5h	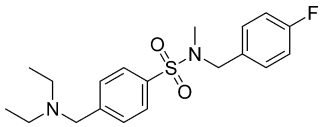	1000	61	82
5i	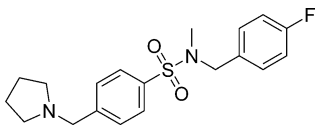	1000	64	99

ed sulfonamide motif as potential CXCR4 blockers using the preliminary and less time-consuming EC binding assay. Thus, the molecular sectors to the left (region A) and to the right (region B) of the mono-substituted sulfonamide structure **5b** (Figure 3) were

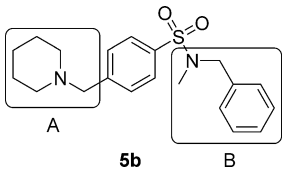

Figure 3. Two regions (A and B) modified for preliminary structure–activity pattern.

explored by substitution and binding affinity screening against **2**. The central phenyl ring was left untouched, as previous work in our research group has shown that this ring is critical for activity.[9a, 10a] Several cyclic and acyclic amines were introduced to region A of the benzenesulfonamide motif (Scheme 2). The morpholine derivative **5c** and the pyrrole derivative **5f** were not well tolerated, and showed EC values >1000 nM. However, the potencies of diethyl (**5d**) and piperazine (**5e**) derivatives were similar to the initially synthesized compounds **5a** and **5b**. Small non-aromatic rings appear to be favored in region A.

Next, region B was explored by adding substituted aromatic rings (fluoro, *tert*-butyl, or methoxy groups) or a pyridine ring, while retaining the piperidine, pyrrolidine, or diethylamine groups in region A. Surprisingly, addition of fluoro or methoxy groups at the *para* position (**5h**, **5i**, and **5l**), as well as *ortho*- and *meta*-fluorine (**5m** and **5n**, respectively), resulted in a significant decrease in binding relative to **5b**. However, addition of a *tert*-butyl moiety to the *para* position produced the potent compounds **5j** and **5k**. Replacement of the phenyl ring of region B with a pyridine ring (compound **7**) likewise enhanced potency. Due to the success of **11a**, additional analogues were prepared that retained the diethylamine fragment in region B, but varied region A with cyclic, acyclic, or aromatic substituents. In this case, the five- and six-membered rings were well tolerated in region A (**11c** and **11d**). However, the morpholine-substituted **11b** showed poor activity, as was the case for the other morpholine analogue **5c**.

Because we used only four concentrations (1, 10, 100, and 1000 nM) for the TN14003 binding assay to determine EC values, we performed seven-point evaluations for several compounds, with EC values ranging from 1 to 1000 nM (Figure 4). The comparative results (Table 2) illustrate that the rhodamine

Table 1. (Continued)

Compound	EC [nM]	Invasion inhib. [%][a] 10 nM	100 nM
5j 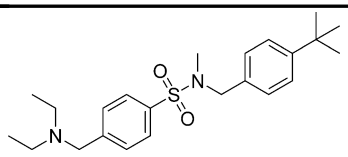	1	40	88
5k 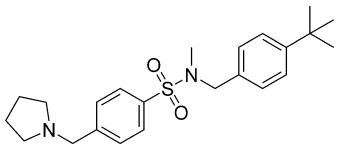	1	20	79
5l 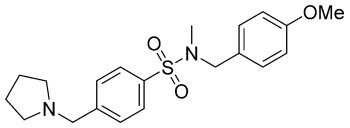	>1000	27	82
5m 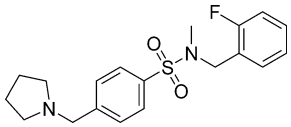	1000	54	98
5n 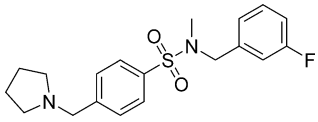	1000	54	88
7 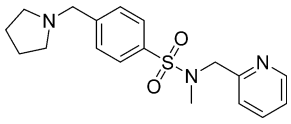	1	39	44
11a 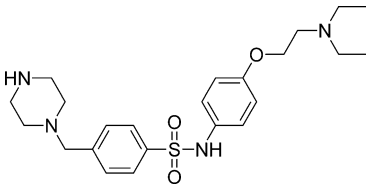	10	77	77
11b 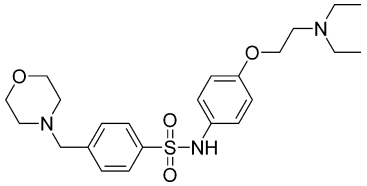	1000	0	37
11c 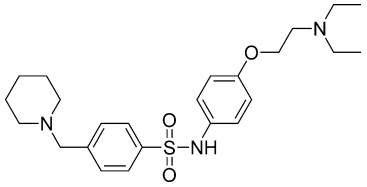	100	17	25
11d 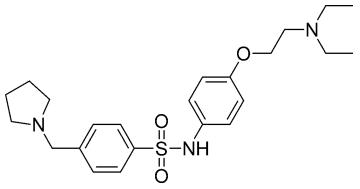	10	34	82

[a] NA: not applicable.

assay is semi-quantitative and able to demonstrate binding at a minimum within a factor of 5–10.

Matrigel invasion assays

The Matrigel invasion assay, a functional probe using full-length CXCL12, was employed as a secondary functional assay to test whether the compounds can block CXCR4/CXCL12-mediated chemotaxis and invasion at two concentrations (10 and 100 nM).[12] The reason for selecting these two concentrations was to identify potent compounds that are reasonably active at least at 100 nM and to show concentration dependence. The results of both binding affinity and Matrigel invasion for all analogues are listed in Table 1 except for compounds showing a binding affinity >1000 nM. We previously demonstrated that the dominant effects of our Matrigel invasion arise from a CXCR4/CXCL12-mediated process.[10b,12] The results show that **5a** and **5b** perform well in both the affinity binding assay and invasion assay at 95–100% inhibition of invasion at 100 nM as compared with antagonist **2** as the positive control (set as 100% inhibition of CXCR4/CXCL12-mediated invasion). Compound **5d** also delivered a reasonable result of 71 and 84% at 10 and 100 nM, respectively. Compound **5g** exhibited a binding affinity of 100 nM, although the results in the Matrigel invasion were moderate at 48% (10 nM) and 72% (100 nM). Compound **5k** showed an EC value of 1 nM in the binding affinity assay and also gave moderate results in the Matrigel invasion assay. For the series **11a–d**, **11a** delivered a satisfying result in both the binding affinity assay (EC = 10 nM) and the Matrigel invasion assays (77% at 10 and 100 nM). Compound **11d** gave a binding affinity EC value of 10 nM and performed moderately in the Matrigel invasion assay, with 82% inhibition of invasion at 100 nM.

One striking feature of the data as it pertains to results across both binding and Matrigel assays is the behavior of six compounds: **3b**, **5c**, **5h**, **5i**, **5m**, and **5n**. Each substance furnishes a binding assay EC value of 1000 nM (Table 1), but a contrary Matrigel invasion decrease of >75%. A consistent proposal for the behavior of this subset (29% of the compounds prepared) is provided below in the context of antagonist orientation in the binding pocket of CXCR4. One final unusual and unique compound is **7**, which evidences a binding concentration of 1 nM, but a Matrigel invasion outcome of 44%. We regard this compound as an outlier that needs further examination.

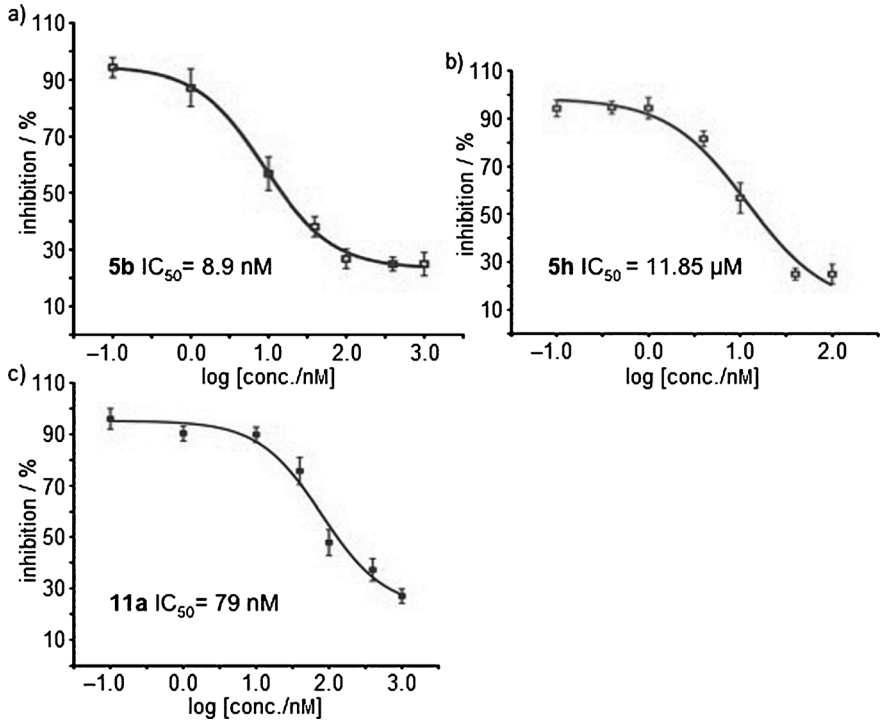

Figure 4. IC_{50} determination curves for selected compounds a) **5b**, b) **5h**, and c) **11a**.

Computational modeling

Mapping CXCR4 antagonists and CXCL12 N-terminal binding sites

Computational docking of the synthesized ligands into the binding pocket of the recently disclosed CXCR4 X-ray structure[13] was performed to furnish insight into the discrepancies between the binding affinities (EC values) and Matrigel invasion assay results for the subset of six analogues mentioned above. Compared with previously solved GPCR X-ray structures, the binding cavity of CXCR4 is larger and more open with a cavity volume of 3322 Å^3.[13] The small-molecule antagonist IT1t only occupies part of the pocket. Several functional studies of mutant CXCR4 revealed that Asp97, Asp187, Glu288, Phe87, Asp171, and Phe292 are required for CXCL12 binding, while the first three residue mutants impair CXCL12 signaling.[14] The cyclic peptides **2** and CVX15 (**12**) are CXCR4 antagonists of known structure. CXCR4 alanine scanning for mutants identified residues required for the binding of **2** to be Asp171, Arg188, Tyr190, Gly207, and Asp262.[15] By combining the mutational outcomes with crystal structure analysis, we can map the binding sites of the CXCR4 antagonists and the CXCL12 N terminus. In this way, antagonist peptides **2** and **12** are shown to occupy similar sectors of the CXCR4 binding cavity, as most of the key residues sensitive to the binding of **2** are in close contact with **12**. However, mutational analysis also shows that the CXCL12 N terminus binds in another sector of the binding pocket, leading to only partial overlap between peptide antagonist and CXCL12 N-terminal binding (Figure 5).

Prediction of benzenesulfonamide analogue binding poses

To explore the possible structural basis behind the binding/Matrigel discrepancy for certain benzenesulfonamides, we arbitrarily classified the analogues of Table 1 as active ($EC \leq 100$ nM) or inactive ($EC \geq 1000$ nM). In general, we found that the unscaled binding free energies from Prime MM-GBSA calculations correlate with the two categories of effective concentrations. For compounds regarded as active, the unscaled energies are $> |30|$ kcal mol^{-1} (Table 3). For example, the best Glide docking pose of **5a** (Figure 6a, $EC = 10$ nM) is protonated on the pyrrolidine nitrogen atom, forms a salt bridge (2.8 Å) to Asp97, and delivers a predicted binding free energy of -36.4 kcal mol^{-1}. One oxygen atom of the sulfonamide engages in a hydrogen bond with Arg188. Both the pyrrolidine and phenyl rings fit into small sub-pockets and make hydrophobic contacts with CXCR4 (Figure 6b).

Superposition of all the docked active analogues suggests that they reside in a similar location and form either a salt bridge or a hydrogen bond with Asp97 or Glu288, which play key roles in CXCL12 binding and signal transduction[14a] (Figure 6c). For compounds classified as binding inactive ($EC \geq 1000$ nM), the unscaled binding free energies are in the range of -10 to -20 kcal mol^{-1}, except for **5h**, **5i**, and **5l**, which fall between -40 and -42 kcal mol^{-1} (Table 3). No polar interactions or hydrogen bonds are formed between the two key CXCR4 residues Asp187 or Glu288 for the latter agents as well as inactive **7**. For selected compounds the IC_{50} values versus docking scores (Table 4) show a trend similar to the EC values versus docking scores (Table 3). Superposition of **5h**, **5i**, and **5l**, all with predicted binding free energies in the highly active range (-40 to -42 kcal mol^{-1}), suggests that these agents associate with CXCR4 in poses that place the structures in a distinct part of the binding pocket near Asp97. The nitrogen atoms of the pyrrolidine groups are protonated and form salt bridges (2.7 Å) to Asp97 (Figure 7). None show overlap with the peptide **12** binding geometry (Figure 5a,d), unlike the actives displayed in Figure 6. Thus, it is suggested that these three compounds bind efficiently to the CXCR4–**12** complex, but are unable to compete with antagonist **2**. This explains the inconsistency between the high experimental 1000 nM concentrations and the substantial calculated binding free energies for **5h**, **5i**, and **5l**, as peptidic antagonist **2** and **12** occupy essentially the same but different sector of the binding pocket

Table 2. Selected sulfonamide analogues evaluated by both single-point binding affinity (EC) and seven-point IC_{50} values.

Compound	EC [nM]	IC_{50} [nM]
5a 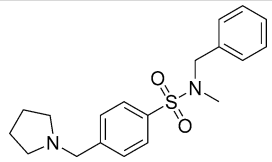	10	8.0
5b 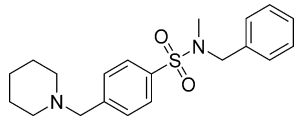	1	8.9
5c 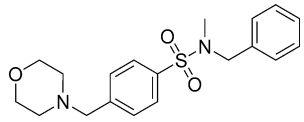	1000	5300
5g 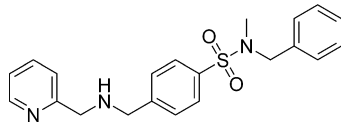	100	113
5h 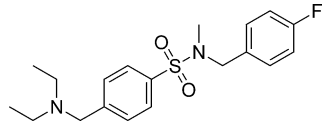	1000	11850
5i 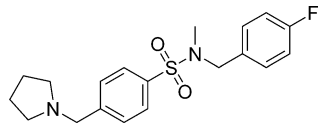	1000	7300
5l 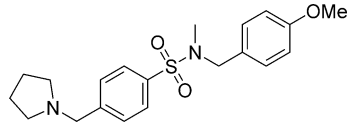	>1000	64900
11a 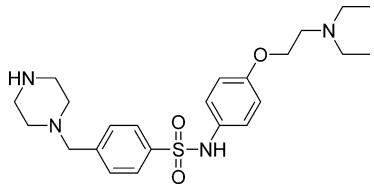	10	79
11c 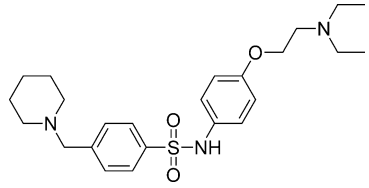	1000	21

(Figure 5c). It may also explain the activities of **3b**, **5h**, and **5i** in the Matrigel invasion assay, which incorporates full-length CXCL12 and overlaps with both sectors of CXCR4 (Figure 5).

A further observation provides additional support for this interpretation, while taking into account a unique structural factor for **5h**, **5i**, and **5l** in terms of the *para*-fluoro or *para*-methoxy groups located within the benzyl substituent. That is, **5h** and its congeners are predicted to adopt alternative poses, as depicted in Figure 7b and Figure 7c. The protonated amine forms a salt bridge with Asp97, consistent with the same interaction for all the active analogues as monitored by the EC binding affinities. In addition, the SO_2 moiety engages in a bifurcated hydrogen bond with Ser285, one face of the fluorophenyl group resides in a hydrophobic environment, and the *para*-fluorine atom is closely associated with cationic Lys38 (Figure 7d). It is well known that organic fluorides enjoy a strong electrostatic interaction with cationic amines sufficient to alter the classic axial/equatorial rules of conformational analysis.[16] While the corresponding *para*-methoxy analogue **5l** can be expected to experience a similar productive interaction with Lys38, the *tert*-butyl analogues **5j** and **5k** do not do so for both steric and electrostatic reasons, adopting the poses shown in Figure 6 instead. In sum, this analysis suggests that the polar *para* substituents provide an unexpected anchor site, altering the binding pose while directing the compounds away from bound **2**.

As a test of the hypothesis regarding the role of aromatic fluorine in reshaping the binding pose, we prepared **5m** and **5n** (Table 1), analogues of **5i** in which the *para*-fluoro substituent was separately moved to the *ortho* and *meta* positions. According to the model of Figure 7d, Arg183 hydrogen bonded to Asp97 is perfectly poised to anchor the aromatic fluoride at these centers, analogous to the action of Lys38 at the *para* position of **5h**. Accordingly, when **5m** and **5n** were subjected to the Matrigel assay at 100 nM, they blocked invasion at 98 and 88%, respectively. This compares with 82 and 99% at the same concentration for **5h** and **5i**, respectively. Such stabilization is not unprecedented. As part of a mechanistic enzyme study, a conformational partition of a CF_3-methionine between two closely spaced arginines in bacteriophage λ lysozyme has been observed by NMR spectroscopy.[17]

Conclusions

We synthesized a novel class of benzenesulfonamides that inhibit CXCR4 as evidenced by the displacement of antagonist TN14003 (**2**) from the receptor. Compounds **5a** and **5b** were among the most potent compounds, and exhibit IC_{50} values of <10 nM in the binding affinity assay and show $>90\%$ inhibition of invasion in the Matrigel invasion assay relative to the control. Computer modeling reveals that the potent analogues interact with key residues Asp97 and Arg188 in the CXCR4 binding pocket, mutations of which interfere with receptor action. In addition, the modeling provides a satisfying explanation for compounds that perform poorly in the binding affinity assay against **2**, but deliver favorable blockade of Matrigel invasion and MM-GBSA binding free energies reflecting good to excellent potency. The binding/Matrigel inconsistency is resolved by the observation that these compounds are predicted to dock in the CXCL12 binding region, but, in the expansive binding site, do not overlap with **2** and thus do not compete with it. It is unusual for two drug-sized molecules to bind simultaneously to the same binding site. However, the muscarinic M2 receptor[18] and the sweet receptor[19] may be two examples of the phenomenon exemplified by Figure 7b. Unfortunately, these results suggest that the utility of the EC binding site assay would appear to be compromised as a primary

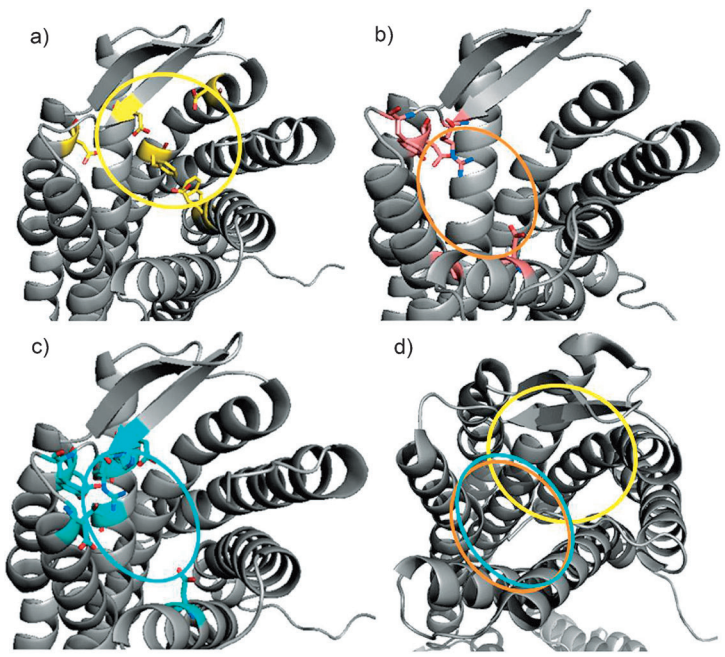

Figure 5. Mapping the location of peptide ligands onto the CXCR4 binding cavity based on X-ray structure and point mutations sensitive to ligand binding. a) CXCL12 N terminus (yellow circle); b) peptidic antagonist **2** (orange circle); c) CVX15 (**12**) (cyan circle); d) superposition of CXCL12, **2**, and **12** binding sites.

Table 3. Effective concentration and predicted relative binding free energies for active and inactive compounds.

Active Compd	EC [nM]	MM-GBSA [kcal mol^{-1}]	Inactive Compd	EC [nM]	MM-GBSA [kcal mol^{-1}]
5b	1	−37.4	**3a**	1000	−21.5
5j	1	−31.4	**3b**	1000	−20.7
5k	1	−29.7	**3c**	1000	−13.4
7	1	−40.3	**5f**	1000	−15.0
5e	1	−31.7	**5h**	1000	−42.1
5a	10	−36.4	**5i**	1000	−40.0
11a	10	−34.5	**5l**	1000	−40.3
5d	10	−33.5			

screen for CXCR4 antagonists, and, at the very least, needs to be complemented by a second functional assay.

Experimental Section

Initial screening of anti-CXCR4 small molecules based on a binding affinity assay

Binding affinity and cell invasion assays are basic tools that apply to the initial screening. MDA-MB-231 cells cultured in an eight-well slide chamber were pre-incubated with the test compounds at 1, 10, 100, and 1000 nM. The cells were fixed with 4% formaldehyde and incubated with 50 nM biotinylated **2** followed by rhodamine staining.

IC_{50} measurement for select sulfonamide analogues: IC_{50} values of selected compounds were tested at 1, 4, 10, 40, 100, 400, and 1000 nM, or at 0.1, 0.4, 1, 4, 10, 40, and 100 μM, based on the results of initial screening. MDA-MB-231 cells (2×10^4) were cultured in an eight-well slide chamber for two days. The cells were pre-incubated with the test compounds for 15 min, and then the cells were fixed with 4% formaldehyde. The fixed cells were subsequently incubated for 45 min with biotinylated **2** (50 ng mL^{-1}).[10b,12] Cells were incubated for 30 min in streptavidin–rhodamine at a 1:150 dilution (Jackson Immuno Research Laboratories, West Grove, PA, USA) after washing three times with PBS. Finally, the slides were washed with PBS and mounted in an anti-fade mounting solution (Molecular Probes, Eugene, OR, USA). Five pictures of stained cells for each treatment were taken on a Nikon Eclipse E800 microscope. Pictures were analyzed quantitatively with ImageJ, and IC_{50} values for each compound were fitted with GraphPad Prism 4.

Matrigel cell invasion assays

Matrigel invasion chambers from BD Biocoat Cellware (San Jose, CA, USA) were used for invasion assays. MDA-MB-231 cells were cultured on a layer of Matrigel in the upper chamber with test compounds at 10 or 100 nM, while 200 ng mL^{-1} CXCL12 was added in the lower chamber as a chemoattractant. Detailed procedures for the binding affinity and invasion assays have been described in previous publications.[2c,10b,12]

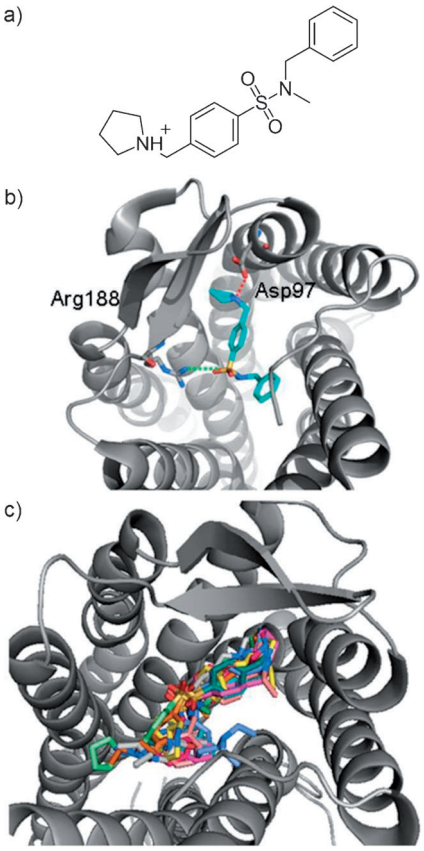

Figure 6. a) Structure of **5a**; b) best docking pose for **5a** in the CXCR4 binding pocket; c) superposition of the Glide/MM-GBSA best binding poses in CXCR4 for all active analogues.

Table 4. IC_{50} (binding affinity assay) determination of selected compounds and the corresponding docking score.

Compound	IC_{50} [nM]	MM-GBSA [kcal mol^{-1}]
5j 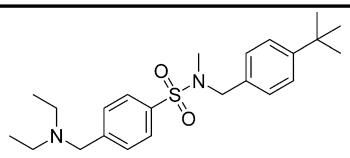	4.6	−31.4
5a 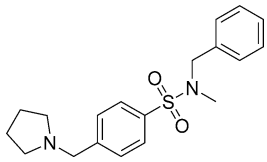	8.0	−36.4
11c 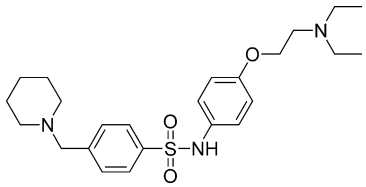	21.1	−31.4
5c 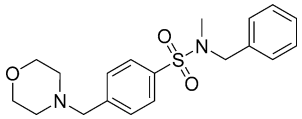	5285	−13.4
5f 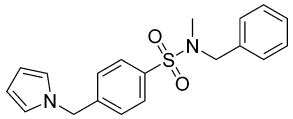	9849	−15.0
5i 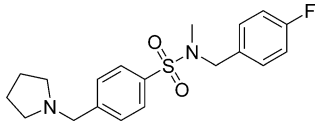	30359	−40.0

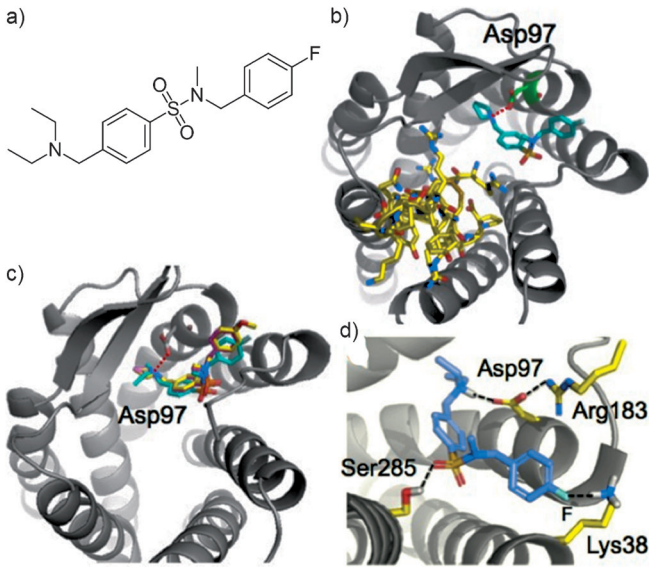

Figure 7. a) Structure of **5h**; b) best docking pose of **5i** (cyan) in CXCR4 with X-ray position of **12** (yellow); c) superposition of best binding poses of protonated **5h** (cyan), **5i** (magenta), and **5l** (yellow) in CXCR4; d) close-up view of protonated **5h** showing key interactions with residues on adjacent helices in the binding site. The conformation of Lys38 was established by conformational searching of its side chain following docking of **5h**.

Computational protein–ligand docking

The acid dissociation constant (pK_a) of the benzenesulfonamide derivatives was predicted by ACD software.[20] Based on these values, nitrogen sites in these compounds were protonated when the pK_a was estimated to be >7. All prepared benzenesulfonamide derivatives with the appropriate N site protonated were docked flexibly into the cavity region of the human chemokine receptor CXCR4 crystal structure (PDB code: 3ODU) devoid of the small-molecule antagonist IT1t using Glide with standard precision (Schrödinger, LLC).[21] This methodology regards the protein structure as a rigid body, but treats the ligand as a conformationally flexible molecule. The resulting CXCR4–benzenesulfonamide complexes were subsequently sorted energetically with the MM-GBSA scoring algorithm, which provides an estimate of relative binding free energies.[22] The volume of the CXCR4 cavity was obtained by the web-based CASTp package.[23]

Chemistry

General: ^{1}H and ^{13}C NMR spectra were recorded on an INOVA-400 (400 MHz) spectrometer. The spectra obtained in $CDCl_3$ or [D_6]DMSO was referenced to the residual solvent peak. Chemical shifts (δ) are reported in parts per million (ppm) relative to residual non-deuterated solvent as an internal reference. The following abbreviations are used to explain the multiplicities: s = singlet, d = doublet, t = triplet, q = quartet, dd = doublet of doublets, dt = doublet of triplets, m = multiplet, br = broad. Mass spectra were recorded on a JEOL spectrometer at Emory University Mass Spectrometry Center.

General procedure for the synthesis of 3: To a solution of xylylenediamine (1 equiv) in CH_2Cl_2 was added DIPEA (2 equiv) and the appropriate sulfonyl chloride (2 equiv). The reaction mixture was stirred at room temperature for 3 h. The white precipitate was filtered and washed with CH_2Cl_2 to give the product as white crystals.

***N,N′*-[1,4-Phenylenebis(methylene)]dibenzenesulfonamide (3a)**: White crystals (527 mg, 34%): ^{1}H NMR (400 MHz, $CDCl_3$): $\delta = 8.22$ (s, 2H), 7.84 (d, $J = 8.0$ Hz, 2H), 7.62 (m, 6H), 7.13 (s, 4H), 3.89 ppm (s, 4H); ^{13}C NMR (400 MHz, [D_6]DMSO): $\delta = 140.7$, 136.6, 132.34, 129.19, 127.44, 126.44, 45.8 ppm; HRMS: m/z $[M+H]^+$ calcd for $C_{20}H_{20}N_2O_4S_2$: 415.07917, found: 415.07879.

***N,N′*-[1,4-Phenylenebis(methylene)]bis(4-methoxybenzenesulfonamide) (3b)**: White crystals (562 mg 60%): ^{1}H NMR (400 MHz, [D_6]DMSO): $\delta = 7.94$ (br s, 2H), 7.73 (d, $J = 8.8$ Hz, 4H), 7.14 (s, 4H), 7.10 (d, $J = 9.2$ Hz, 4H), 3.88 (s, 4H), 3.83 ppm (s, 6H); ^{13}C NMR (400 MHz, [D_6]DMSO): $\delta = 162.1$, 136.6, 132.3, 128.7, 127.4, 114.3, 55.62, 45.8 ppm; HRMS: m/z $[M+H]^+$ calcd for $C_{22}H_{24}N_2O_6S_2$: 477.11486, found: 477.11457.

General procedure for the synthesis of 4: To a solution of 4-(bromomethyl)benzene-1-sulfonyl chloride (1 equiv) in CH_2Cl_2 (0.1 M) was added the amine (2 equiv). The reaction mixture was allowed to stir at room temperature for 2 h to overnight. The reaction mixture was washed with H_2O and brine, and the combined organic layers were dried over $MgSO_4$ and concentrated to give the final compound.

***N*-Benzyl-4-(bromomethyl)-*N*-methylbenzenesulfonamide (4a)**: Off-white solid, (116 mg, 20%): ^{1}H NMR (400 MHz, $CDCl_3$): $\delta = 7.84$ (d, $J = 8.0$ Hz, 2H), 7.59 (d, $J = 8.0$ Hz, 2H), 7.34–7.31 (m, 5H), 4.65 (s, 2H), 4.16 (s, 2H), 2.61 ppm (s, 3H); ^{13}C NMR (400 MHz, $CDCl_3$): $\delta = 142.7$, 137.6, 135.6, 130.0, 129.4, 128.9, 128.5, 128.2, 128.1, 54.3,

34.5, 31.8 ppm; HRMS: *m/z* $[M+H]^+$ calcd for $C_{15}H_{15}BrN_2O_2SNa$: 376.9930, found: 376.9932.

4-(Bromomethyl)-*N*-(4-fluorobenzyl)-*N*-methylbenzenesulfonamide (4b): White powder (235 mg, 32%): ^{1}H NMR (400 MHz, $CDCl_3$): δ = 7.81 (d, J = 8.4 Hz, 2H), 7.58 (d, J = 8.4 Hz, 2H), 7.27 (d, J = 8.4 Hz, 2H), 7.03 (d, J = 8.4 Hz, 2H), 4.53 (s, 2H), 4.13 (s, 2H), 2.61 ppm (s, 3H); HRMS: *m/z* $[M+H]^+$ calcd for $C_{15}H_{17}N_2O_2F_1S_1$: 372.0065, found: 372.0064.

4-(Bromomethyl)-*N*-(4-(*tert*-butyl)benzyl)-*N*-methylbenzenesulfonamide (4c): White powder (686 mg, 90%): ^{1}H NMR (400 MHz, $CDCl_3$): δ = 7.81 (d, J = 8.4 Hz, 2H), 7.57 (d, J = 8.4 Hz, 2H), 7.35 (d, J = 8.8 Hz, 2H), 7.21 (d, J = 8.4 Hz, 2H), 4.53 (s, 2H), 4.13 (s, 2H), 2.62 (s, 3H), 1.31 ppm (s, 9H); ^{13}C NMR (400 MHz, $CDCl_3$): δ = 151.2, 142.7, 137.7, 132.5, 129.9, 128.3, 128.2, 125.8, 53.9, 34.7, 34.5, 31.8, 31.5, 31.36 ppm; HRMS: *m/z* $[M+H]^+$ calcd for $C_{19}H_{24}NO_2BrNaS$: 432.0603, found: 432.0607.

4-(Bromomethyl)-*N*-(4-methoxybenzyl)-*N*-methylbenzenesulfonamide (4d): Off-white powder (581 mg, 81%): ^{1}H NMR (400 MHz, $CDCl_3$): δ = 7.81 (d, J = 8.4 Hz, 2H), 7.57 (d, J = 8.8 Hz, 2H), 7.20 (d, J = 8.8 Hz, 2H), 6.86 (d, J = 8.4 Hz, 2H), 4.53 (s, 2H), 4.10 (s, 2H), 3.80 (s, 3H), 2.59 ppm (s, 3H); ^{13}C NMR (400 MHz, $CDCl_3$): δ = 159.6, 142.7, 137.6, 132.1, 129.9, 129.4, 128.1, 127.5, 114.7, 114.3, 55.5, 53.7, 34.3, 31.8 ppm; HRMS: *m/z* $[M+H]^+$ calcd for $C_{16}H_{18}NO_3BrNaS$: 406.0083, found: 406.0093.

General procedure for the synthesis of 5: To a solution of **4** (1 equiv) in CH_3CN was added K_2CO_3 (2 equiv) and the amine (1 equiv). The reaction mixture was allowed to stir at room temperature overnight. The organic solvent was removed by rotary evaporation, and the residue was dissolved in CH_2Cl_2 and washed with H_2O and brine, dried over $MgSO_4$, and concentrated. The crude product was purified by column chromatography.

***N*-Benzyl-*N*-methyl-4-(pyrrolidin-1-ylmethyl)benzenesulfonamide (5a)**: Off-white solid, (52 mg, 41%): ^{1}H NMR (400 MHz, $CDCl_3$): δ = 7.81 (d, J = 8.4 Hz, 2H), 7.58 (d, J = 8.4 Hz, 2H), 7.31–7.27 (m, 5H), 4.15 (s, 2H), 3.74 (s, 2H), 2.60 (s, 7H), 1.85 ppm (m, 4H); ^{13}C NMR (400 MHz, $CDCl_3$): δ = 136.0, 135.9, 129.6, 128.9, 128.6, 128.1, 127.7, 60.3, 54.5, 54.3, 34.6, 23.7 ppm; ^{13}C NMR (400 MHz, $CDCl_3$): δ = 144.6, 135.8, 135.7, 129.3, 128.6, 128.3, 127.9, 127.5, 60.1, 54.3, 54.1, 34.3, 29.7, 23.5 ppm; HRMS: *m/z* $[M+H]^+$ calcd for $C_{19}H_{25}N_2O_2S$: 345.16313, found: 345.16296.

***N*-Benzyl-*N*-methyl-4-(piperidin-1-ylmethyl)benzenesulfonamide (5b)**: Off-white solid (40 mg, 30%): ^{1}H NMR (400 MHz, $CDCl_3$): δ = 7.76 (d, J = 8.8 Hz, 2H), 7.50 (d, J = 8.4 Hz, 2H), 7.29 (m, 5H), 4.13 (s, 2H), 3.53 (s, 2H), 2.58 (s, 3H), 2.38 (s, 4H), 1.58 (q, J = 5.4 Hz, 4H), 1.42 ppm (br s, 2H); ^{13}C NMR (400 MHz, $CDCl_3$): δ = 136.2, 135.8, 131.1, 129.9, 128.8, 128.6, 128.1, 127.6, 63.1, 54.8, 54.3, 38.9, 34.6, 30.5, 29.1, 25.9, 24.2, 23.9, 23.2, 14.2, 11.2 ppm; HRMS: *m/z* $[M+H]^+$ calcd for $C_{20}H_{27}N_2O_2S$: 359.17878, found: 359.17856.

***N*-Benzyl-*N*-methyl-4-(morpholinomethyl)benzenesulfonamide (5c)**: White solid (86 mg, 57%): ^{1}H NMR (400 MHz, $CDCl_3$): δ = 7.78 (d, J = 8.4 Hz, 2H), 7.52 (d, J = 8.4 Hz, 2H), 7.31–7.24 (m, 5H), 4.13 (s, 2H), 3.71 (t, J = 4.4 Hz, 4H), 3.59 (s, 2H), 2.59 (s, 3H), 2.46 ppm (t, J = 4.8 Hz, 4H); ^{13}C NMR (400 MHz, $CDCl_3$): δ = 143.5, 136.2, 135.6, 129.5, 128.7, 128.4, 127.9, 127.6, 67.0, 62.7, 54.1, 53.7, 34.4 ppm; HRMS: *m/z* $[M+H]^+$ calcd for $C_{19}H_{25}N_2O_3S$: 361.1580, found: 361.1581.

***N*-Benzyl-4-[(diethylamino)methyl]-*N*-methylbenzenesulfonamide (5d)**: White solid (117 mg, 60%): ^{1}H NMR (400 MHz, $CDCl_3$): δ = 7.77 (d, J = 8.4 Hz, 2H), 7.58 (d, J = 8.4 Hz, 2H), 7.28 (m, 5H), 4.13 (s, 2H), 3.70 (s, 2H), 2.59 (m, 7H), 1.09 ppm (t, J = 7.0 Hz, 6H); ^{13}C NMR (400 MHz, $CDCl_3$): δ = 144.3, 136.2, 135.7, 129.8, 128.8, 128.5, 128.0, 127.6, 57.0, 54.2, 47.0, 34.5, 11.4 ppm; HRMS: *m/z* $[M+H]^+$ calcd for $C_{19}H_{27}N_2O_2S$ 347.1788, found: 347.1787.

***N*-Benzyl-*N*-methyl-4-(piperazin-1-ylmethyl)benzenesulfonamide (5e)**: White solid, (141 mg, 46%): ^{1}H NMR (400 MHz, $CDCl_3$): δ = 7.72 (d, J = 8.4 Hz, 2H), 7.46 (d, J = 8.8 Hz, 2H), 7.28–7.19 (m, 5H), 4.08 (s, 2H), 3.51 (s, 2H), 2.86 (t, J = 4.8 Hz, 4H), 2.54 (s, 3H), 2.39 ppm (br s, 4H); ^{13}C NMR (400 MHz, $CDCl_3$): δ = 141.3, 136.2, 135.4, 128.2, 128.8, 128.1, 127.6, 126.9, 64.2, 57.0, 54.7, 46.3, 34.9 ppm; HRMS: *m/z* $[M+H]^+$ calcd for $C_{19}H_{26}N_3O_2S$: 360.1740, found: 360.1741 $[M+H]^+$.

4-[(1*H*-Pyrrol-1-yl)methyl]-*N*-benzyl-*N*-methylbenzenesulfonamide (5f): White powder (103 mg, 53%): ^{1}H NMR (400 MHz, $CDCl_3$): δ = 7.77 (dd, J = 2.0, 8.0 Hz, 2H), 7.32–7.21 (m, 7H), 6.70 (t, J = 2.0 Hz, 2H), 6.23 (t, J = 2.4 Hz, 2H), 5.16 (s, 2H), 4.23 (s, 2H), 2.56 ppm (s, 3H); ^{13}C NMR (400 MHz, $CDCl_3$): δ = 143.6, 136.9, 135.7, 128.9, 128.5, 128.1, 127.5, 121.4, 109.4, 54.3, 52.9, 34.5 ppm; HRMS: *m/z* $[M+H]^+$ calcd for $C_{19}H_{21}N_2O_2S$: 341.1318, found: 341.1316.

***N*-Benzyl-*N*-methyl-4-{[(pyridin-2-ylmethyl)amino]methyl}benzenesulfonamide (5g)**: Yellow solid (14 mg, 21%): ^{1}H NMR (400 MHz, $CDCl_3$): δ = 8.56 (d, J = 4.0 Hz, 1H), 7.79 (d, J = 8.0 Hz, 2H), 7.66 (td, J = 8.0, 1.6 Hz, 1H), 7.34–7.24 (m, 6H), 7.20–7.17 (m, 1H), 4.12 (s, 2H), 3.96 (s, 2H), 3.95 (s, 2H), 2.57 ppm (s, 3H); ^{13}C NMR (400 MHz, $CDCl_3$): δ = 159.2, 149.4, 145.6, 144.5, 136.7, 135.9, 135.7, 129.4, 129.4, 129.4, 128.9, 128.7, 128.5, 128.0, 127.7, 127.6, 122.6, 122.3, 122.0, 58.1, 54.5, 54.2, 52.9, 34.5, 29.8 ppm; HRMS: *m/z* $[M+H]^+$ calcd for $C_{21}H_{24}N_3O_2S$: 382.1584, found: 382.1582.

4-[(Diethylamino)methyl]-*N*-(4-fluorobenzyl)-*N*-methylbenzenesulfonamide (5h): White solid (45 mg, 59%): ^{1}H NMR (400 MHz, $CDCl_3$): δ = 7.77 (d, J = 8.4 Hz, 2H), 7.60 (d, J = 8.4 Hz, 2H), 7.26 (t, J = 7.4 Hz, 2H), 7.02 (t, J = 7.0 Hz, 2H), 4.12 (s, 2H), 3.65 (s, 2H), 2.60–2.55 (m, 7H), 1.07 ppm (t, J = 7.2 Hz, 6H); ^{13}C NMR (400 MHz, $CDCl_3$): δ = 161.0, 135.8, 131.6, 130.3, 130.2, 129.5, 127.6, 115.9, 115.7, 57.4, 53.6, 47.2, 34.5, 12.0 ppm; HRMS: *m/z* $[M+H]^+$ calcd for $C_{19}H_{26}N_3FO_2S$: 365.1694, found: 365.1690.

***N*-(4-Fluorobenzyl)-*N*-methyl-4-(pyrrolidin-1-ylmethyl)benzenesulfonamide (5i)**: Yellow solid (42 mg, 57%): ^{1}H NMR (400 MHz, $CDCl_3$): δ = 7.76 (d, J = 8.0 Hz, 2H), 7.52 (d, J = 8.0 Hz, 2H), 7.25 (t, J = 8.4, 2H), 7.00 (d, J = 8.4 Hz, 2H), 4.09 (s, 2H), 3.69 (s, 2H), 2.57–2.51 (m, 7H), 1.80 ppm (br s, 4H); ^{13}C NMR (400 MHz, $CDCl_3$): δ = 145.0, 136.0, 131.6, 130.3, 130.2, 129.6, 127.7, 115.9, 115.7, 60.3, 54.5, 53.6, 34.5, 23.7 ppm; HRMS: *m/z* $[M+H]^+$ calcd for $C_{19}H_{24}N_2FO_2S$: 363.1537, found: 363.1534.

***N*-[4-(*tert*-Butyl)benzyl]-4-[(diethylamino)methyl]-*N*-methylbenzenesulfonamide (5j)**: White solid (54 mg, 56%). NMR (400 MHz, $CDCl_3$): δ = 7.80 (d, J = 8.4 Hz, 2H), 7.57 (d, J = 8.4 Hz, 2H), 7.37 (d, J = 8.0 Hz, 2H), 7.25 (d, J = 8.4 Hz, 2H), 4.15 (s, 2H), 3.67 (s, 2H), 2.63 (s, 3H), 2.58 (q, J = 7.2 Hz, 4H), 1.34 (s, 9H), 1.09 ppm (t, J = 7.2 Hz, 6H); ^{13}C NMR (400 MHz, $CDCl_3$): δ = 151.1, 146.1, 135.9, 132.8, 129.4, 128.3, 127.6, 125.7, 57.4, 53.9, 47.2, 34.7, 34.5, 31.5, 29.9, 12.01 ppm; HRMS: *m/z* $[M+H]^+$ calcd for $C_{23}H_{35}N_2O_2S$ 403.2414, found: 403.2418.

***N*-[4-(*tert*-Butyl)benzyl]-*N*-methyl-4-(pyrrolidin-1-ylmethyl)benzenesulfonamide (5k)**: White powder (51 mg, 55%): ^{1}H NMR (400 MHz, $CDCl_3$): δ = 7.77 (d, J = 8.4 Hz, 2H), 7.54 (d, J = 8.4 Hz, 2H), 7.32 (s, J = 8.4 Hz, 2H), 7.19 (d, J = 8.0 Hz, 2H), 4.10 (s, 2H), 3.72 (s, 2H), 2.58 (s, 7H), 1.83 (s, 4H), 1.24 ppm (s, 9H); ^{13}C NMR (400 MHz, $CDCl_3$): δ = 151.1, 136.3, 132.7, 129.7, 128.3, 127.8, 125.7,

60.1, 54.5, 53.9, 34.7, 34.5, 31.5, 29.9, 23.7 ppm; HRMS: *m/z* $[M+H]^+$ calcd for $C_{23}H_{33}N_2O_2S$: 403.2257, found: 403.2261.

***N*-(4-Methoxybenzyl)-*N*-methyl-4-(pyrrolidin-1-ylmethyl)benzenesulfonamide (5l)**: Yellow powder (142 mg, 77%): ^{1}H NMR (400 MHz, $CDCl_3$): $\delta=7.81$ (d, $J=8.4$ Hz, 2H), 7.53 (d, $J=8.4$ Hz, 2H), 7.20 (d, $J=8.4$ Hz, 2H), 6.85 (d, $J=8.4$ Hz, 2H), 4.07 (s, 2H), 3.79 (s, 2H), 3.70 (s, 3H), 2.56–2.52 (m, 7H), 1.83–1.80 ppm (m, 4H); ^{13}C NMR (400 MHz, $CDCl_3$): $\delta=159.5$, 145.0, 136.0, 129.9, 129.5, 127.7, 114.2, 60.3, 55.5, 54.5, 53.8, 34.3, 29.9, 23.7 ppm; HRMS: *m/z* $[M+H]^+$ calcd for $C_{20}H_{27}N_2O_3S$: 375.1737, found: 375.1737.

***N*-(2-Fluorobenzyl)-*N*-methyl-4-(pyrrolidin-1-ylmethyl)benzenesulfonamide (5m)**: White powder (84 mg, 63%): ^{1}H NMR (400 MHz, $CDCl_3$): $\delta=7.71$ (d, $J=8.0$ Hz, 2H), 7.52 (d, $J=8.4$ Hz, 2H), 7.41 (td, $J=8.0$, 1.6 Hz, 1H), 7.22–7.19 (m, 1H), 7.09 (t, $J=7.2$ Hz, 1H), 6.95 (t, $J=10$ Hz, 1H), 4.18 (s, 2H), 3.71 (s, 2H), 2.60–2.57 (m, 7H), 1.79 ppm (s, 4H); ^{13}C NMR (400 MHz, $CDCl_3$): $\delta=160.1$, 139.8, 136.2, 130.9, 129.9, 127.8, 124.7, 122.8, 115.7, 59.9, 54.4, 47.2, 34.9, 23.7 ppm; HRMS: *m/z* $[M+H]^+$ calcd for $C_{19}H_{23}O_2N_2F$: 363.1537, found: 363.1536.

***N*-(3-Fluorobenzyl)-*N*-methyl-4-(pyrrolidin-1-ylmethyl)benzenesulfonamide (5n)**: White powder (113 mg, 85%): ^{1}H NMR (400 MHz, $CDCl_3$): $\delta=7.71$ (d, $J=6.8$ Hz, 2H), 7.49 (d, $J=8.4$ Hz, 2H), 7.23–7.20 (m, 1H), 7.02–6.91 (m, 3H), 4.07 (s, 2H), 3.66 (s, 2H), 2.55 (s, 3H), 2.51 (br s, 4H), 1.76 ppm (t, $J=6.8$ Hz, 4H); ^{13}C NMR (400 MHz, $CDCl_3$): $\delta=162.5$, 139.8, 137.0, 128.9, 127.8, 127.0, 123.2, 118.8, 113.7, 60.0, 54.3, 59.2, 34.8, 23.7 ppm; HRMS: *m/z* $[M+H]+$ calcd for $C_{19}H_{23}O_2N_2F$: 363.1537, found: 363.1536 $[M+H]^+$.

4-(Bromomethyl)-*N*-methyl-*N*-(pyridin-2-ylmethyl)benzenesulfonamide (6): Follows the same general procedure as for the synthesis of **4**. The crude product was used without further purification (1.24 g, 94%): ^{1}H NMR (400 MHz, [D$_6$]DMSO): $\delta=8.52$ (d, $J=4.4$ Hz, 1H), 7.90–7.82 (m, 3H), 7.71 (d, $J=8.4$ Hz, 2H), 7.45 (d, $J=8.0$ Hz, 1H), 7.38–7.34 (m, 1H), 4.86 (s, 2H), 4.30 (s, 2H), 2.70 ppm (s, 3H); ^{13}C NMR (400 MHz, $CDCl_3$): $\delta=155.5$, 148.2, 142.7, 128.3, 136.7, 129.7, 127.6, 123.2, 122.6, 54.5, 44.9, 35.5 ppm; HRMS: *m/z* $[M+Na]^+$ calcd for $C_{14}H_{15}N_2O_2BrNaS$: 376.9930, found: 376.9928.

***N*-Methyl-*N*-(pyridin-2-ylmethyl)-4-(pyrrolidin-1-ylmethyl)benzenesulfonamide (7)**: Follows the general procedure as for the synthesis of **5**. The crude product was purified by column chromatography (20:1 CH_2Cl_2/MeOH) to give the final compound as a brown oil (72.5 mg, 50%): ^{1}H NMR (400 MHz, $CDCl_3$): $\delta=8.47$ (m, 1H), 7.77 (d, $J=8.4$ Hz, 2H), 7.71 (td, $J=8.0$, 2.0 Hz, 2H), 7.56–7.52 (m, 2H), 7.20–7.18 (m, 2H), 4.29 (s, 2H), 3.73 (s, 2H), 2.69 (s, 3H), 2.57 (s, 4H), 1.84 ppm (s, 4H); ^{13}C NMR (400 MHz, $CDCl_3$): $\delta=156.6$, 149.3, 145.1, 137.3, 135.8, 129.6, 127.7, 122.9, 122.6, 60.2, 56.3, 54.4, 35.5, 23.7 ppm; HRMS: *m/z* $[M+H]^+$ calcd for $C_{18}H_{24}N_3O_2S$: 346.158, found: 346.1584.

***tert*-Butyl 4-[2-(diethylamino)ethoxy]phenylcarbamate 8**: To a solution of *tert*-butyl-4-hydroxyphenylcarbamate (2 g, 9.56 mmol) in DMF (20 mL) was added 2-chloro-*N*,*N*-diethylethanamine (1.97 g, 11.48 mmol) and NaOH (0.96 g, 23.9 mmol). The reaction mixture was stirred at room temperature for 3 h. The reaction mixture was filtered, and the filtrate was diluted with CH_2Cl_2 (20 mL). The organic layer was washed with brine (2×100 mL), dried over $MgSO_4$, and concentrated. The crude product was purified by column chromatography, silica gel, CH_2Cl_2/MeOH (9:1) to give a brown solid (1.99 g, 60%): ^{1}H NMR (400 MHz, $CDCl_3$): $\delta=7.22$ (d, $J=8.9$ Hz, 2H), 6.75 (d, $J=9.2$ Hz, 2H), 4.14 (t, $J=5.6$ Hz, 2H), 3.09 (t, $J=5.2$ Hz, 2H), 2.88 (q, $J=7.2$ Hz, 4H), 1.44 (s, 9H), 6.08 ppm (t, $J=7.2$ Hz, 6H).

4-[2-(Diethylamino)ethoxy]benzenamine (9): To a solution of **8** (1.99 g, 6.46 mmol) in dioxane (10 mL) in an ice bath was added 4 M HCl in dioxane (3 mL). The reaction was allowed to stir overnight and warmed to room temperature. Et_2O was added to the reaction mixture, and the white precipitate was filtered to give product (1.49 g, 51%): ^{1}H NMR (400 MHz, $CDCl_3$): $\delta=6.74$ (d, $J=8.8$ Hz, 2H), 6.63 (d, $J=8.8$ Hz, 2H), 4.00 (t, $J=6.4$ Hz, 2H), 2.87 (t, $J=6.4$ Hz, 2H), 2.66 (q, $J=7.2$ Hz, 4H), 1.08 ppm (t, $J=6.8$ Hz, 6H).

4-(Bromomethyl)-*N*-{4-[2-(diethylamino)ethoxy]phenyl}benzenesulfonamide (10): To a solution of 4-(bromomethyl)benzene-1-sulfonyl chloride (823 mg, 3.0 mmol) in DMF (15 mL) was added **9** (635 mg, 3.0 mmol); the mixture was allowed to stir at room temperature overnight. The reaction mixture was diluted with CH_2Cl_2 (20 mL), washed with H_2O (2×100 mL) and brine (1×100 mL), dried over $MgSO_4$, and concentrated. The crude product was purified by column chromatography, silica gel, CH_2Cl_2/MeOH (15:1 → 10:1 → 5:1) to give an off-white solid (1.27 g, 90%): ^{1}H NMR (400 MHz, $CDCl_3$): $\delta=7.70$ (d, $J=8.4$ Hz, 2H), 7.41 (d, $J=8.0$ Hz, 2H), 6.98 (d, $J=8.8$ Hz, 2H), 6.65 (d, $J=9.2$ Hz, 2H), 4.55 (d, $J=6.0$ Hz, 2H), 4.36 (t, $J=4.6$ Hz, 2H), 3.47 (t, $J=4.4$ Hz, 2H), 3.26 (br s, 4H), 1.39 ppm (t, $J=7.2$ Hz, 6H); HRMS: *m/z* $[M+H]^+$ calcd for $C_{19}H_{26}N_2O_3SBr$: 441.0842, found: 441.0847.

General procedure for the synthesis of 11: A solution of **10** (1 equiv) and secondary amine (1 equiv) in CH_2Cl_2 was stirred at room temperature overnight. The solvent was removed by rotary evaporation, and the crude product was purified by column chromatography (silica gel 9:1 → 6:1 CH_2Cl_2/MeOH).

***N*-{4-[2-(Diethylamino)ethoxy]benzyl}-4-(piperazin-1-ylmethyl)-benzenesulfonamide (11a)**: Brown oil (245 mg, 20%): ^{1}H NMR (400 MHz, $CDCl_3$): $\delta=7.61$ (d, $J=8.4$ Hz, 2H), 7.35 (d, $J=8.0$ Hz, 2H), 6.94 (d, $J=8.8$ Hz, 2H), 6.72 (d, $J=9.2$ Hz, 2H), 3.97 (t, $J=6.0$ Hz, 2H), 3.49 (s, 2H), 2.92 (q, $J=4.8$ Hz, 4H), 2.84 (t, $J=6.0$ Hz, 2H), 2.64 (m, 4H), 2.42 (br s, 4H), 1.07 ppm (t, $J=7.2$ Hz, 6H); ^{13}C NMR (400 MHz, $CDCl_3$): $\delta=143.9$, 136.2, 135.8, 129.7, 129.4, 128.8, 128.6, 128.1, 127.7, 115.2, 63.1, 54.3, 51.8, 48.0, 46.0, 34.5, 29.9,14.3, 11.9 ppm; HRMS: *m/z* $[M+H]^+$ calcd for $C_{23}H_{34}N_4O_3S$: 447.2424, found: 447.2420.

***N*-{4-[2-(Diethylamino)ethoxy]phenyl}-4-(morpholinomethyl)benzenesulfonamide (11b)**: Yellow solid (25 mg, 10%): ^{1}H NMR (400 MHz, $CDCl_3$): $\delta=7.68$ (d, $J=7.6$ Hz, 2H), 7.39 (d, $J=7.6$ Hz, 2H), 7.00 (d, $J=8.0$ Hz, 2H), 6.71 (d, $J=8.4$ Hz, 2H), 4.37 (br s, 2H), 3.70 (t, $J=4.8$ Hz, 4H), 3.51 (s, 2H), 3.20 (br s, 2H), 2.94 (q, $J=7.6$ Hz, 4H), 2.42 (t, $J=4.4$ Hz, 4H), 1.23 ppm (t, $J=8.8$ Hz, 6H); HRMS: *m/z* $[M+H]^+$ calcd for $C_{23}H_{34}N_3O_4S$: 448.2265, found: 448.2261 $[M+H]^+$.

***N*-{4-[2-(Diethylamino)ethoxy]phenyl}-4-(piperidin-1-ylmethyl)-benzenesulfonamide (11c)**: Yellow oil (20 mg, 9%): ^{1}H NMR (400 MHz, $CDCl_3$): $\delta=7.64$ (d, $J=8.4$ Hz, 2H), 7.39 (d, $J=8.0$ Hz, 2H), 6.98 (dt, $J=8.8$, 3.6 Hz, 2H), 6.72 (dt, $J=9.2$, 3.6, 2H), 4.15 (t, $J=5.2$ Hz, 2H), 3.55 (s, 2H), 2.99 (t, $J=8.0$ Hz, 2H), 2.79 (q, $J=6.8$ Hz, 4H), 2.40 (br s, 4H), 1.60 (m, 4H), 1.41 (br s, 2H), 1.10 ppm (t, $J=8.4$ Hz, 6H); ^{13}C NMR (400 MHz, $CDCl_3$): $\delta=156.8$, 143.9, 137.8, 129.6, 127.4, 125.4, 115.1, 66.0, 63.1, 54.6, 51.6, 47.8, 29.8, 25.9, 24.2, 11.2 ppm; HRMS: *m/z* $[M+H]^+$ calcd for $C_{35}H_{36}N_3O_3S$: 448.2265, found: 448.2261.

***N*-(4-(2-(Diethylamino)ethoxy)phenyl)-4-(pyrrolidin-1-ylmethyl)-benzenesulfonamide (11d)**: Yellow semi-solid (40 mg, 19%): ^{1}H NMR (400 MHz, $CDCl_3$): $\delta=7.65$ (d, $J=8.4$ Hz, 2H), 7.37 (d, $J=8.4$ Hz, 2H), 7.00 (d, $J=9.2$ Hz, 2H), 6.72 (d, $J=8.8$ Hz, 2H), 3.96 (t, $J=6.4$ Hz, 2H), 3.61 (s, 2H), 3.25 (s, 2H), 2.83 (t, $J=6.0$ Hz, 2H), 2.61

(q, $J=7.2$ Hz, 4H), 2.48 (t, $J=6.4$ Hz, 4H), 1.77 (br s, 4H), 1.05 ppm (t, $J=6.8$ Hz, 6H); ^{13}C NMR (400 MHz, $CDCl_3$): $\delta=151.7$, 143.9, 137.7, 129.3, 127.6, 125.3, 115.1, 66.2, 60.0, 54.6, 51.6, 47.9, 29.8, 25.9, 23.4, 11.2 ppm; HRMS: m/z $[M+H]^+$ calcd for $C_{23}H_{34}N_3O_4S$: 432.2315, found: 432.2317.

Acknowledgements

We are grateful to Dr. Haipeng Hu for assistance in the preparation of Figure 7d. Grant support: NIH Fellowships in Research and Science Teaching (FIRST) postdoctoral award K12GM000680 (S.R.M.) and NIH R01CA165306 (H.S.).

Keywords: CXCR4 inhibitors · inflammation · metastasis · sulfonamides

[1] a) A. Zlotnik, O. Yoshie, *Immunity* **2000**, *12*, 121 – 127; b) J. J. Campbell, E. C. Butcher, *Curr. Opin. Immunol.* **2000**, *12*, 336 – 341; c) B. A. Zabel, W. W. Agace, J. J. Campbell, H. M. Heath, D. Parent, A. I. Roberts, E. C. Ebert, N. Kassam, S. Qin, M. Zovko, G. J. LaRosa, L. L. Yang, D. Soler, E. C. Butcher, P. D. Ponath, C. M. Parker, D. P. Andrew, *J. Exp. Med.* **1999**, *190*, 1241 – 1256; d) E. C. Butcher, M. Williams, K. Youngman, L. Rott, M. Briskin, *Adv. Immunol.* **1999**, *72*, 209 – 253; e) J. Morales, B. Homey, A. P. Vicari, S. Hudak, E. Oldham, J. Hedrick, R. Orozco, N. G. Copeland, N. A. Jenkins, L. M. McEvoy, A. Zlotnik, *Proc. Natl. Acad. Sci. USA* **1999**, *96*, 14470 – 14475; f) B. Homey, W. Wang, H. Soto, M. E. Buchanan, A. Wiesenborn, D. Catron, A. Muller, T. K. McClanahan, M. C. Dieu-Nosjean, R. Orozco, T. Ruzicka, P. Lehmann, E. Oldham, A. Zlotnik, *J. Immunol.* **2000**, *164*, 3465 – 3470.

[2] a) A. Zlotnik, *Int. J. Cancer* **2006**, *119*, 2026 – 2029; b) G. Lazennec, A. Richmond, *Trends Mol. Med.* **2010**, *16*, 133 – 144; c) Z. X. Liang, Y. H. Yoon, J. Votaw, M. M. Goodman, L. William, H. Shim, *Cancer Res.* **2005**, *65*, 967 – 971; d) Y. Yoon, Z. Liang, X. Zhang, M. Choe, A. Zhu, H. T. Cho, D. M. Shin, M. M. Goodman, Z. G. Chen, H. Shim, *Cancer Res.* **2007**, *67*, 7518 – 7524.

[3] a) M. Zaitseva, A. Blauvelt, S. Lee, C. K. Lapham, V. Klaus-Kovtun, H. Mostowski, J. Manischewitz, H. Golding, *Nat. Med.* **1997**, *3*, 1369 – 1375; b) X. Sanchez, B. Cousins-Hodges, T. Aguilar, P. Gosselink, Z. Lu, J. Navarro, *J. Biol. Chem.* **1997**, *272*, 27529 – 27531; c) Y. Feng, C. C. Broder, P. E. Kennedy, E. A. Berger, *Science* **1996**, *272*, 872 – 877.

[4] A. Müller, B. Homey, H. Soto, N. Ge, D. Catron, M. E. Buchanan, T. McClanahan, E. Murphy, W. Yuan, S. N. Wagner, J. L. Barrera, A. Mohar, E. Verastegui, A. Zlotnik, *Nature* **2001**, *410*, 50 – 56.

[5] A. Peled, I. Petit, O. Kollet, M. Magid, T. Ponomaryov, T. Byk, A. Nagler, H. Ben-Hur, A. Many, L. Shultz, O. Lider, R. Alon, D. Zipori, T. Lapidot, *Science* **1999**, *283*, 845 – 848.

[6] J. A. Belperio, M. P. Keane, D. A. Arenberg, C. L. Addison, J. E. Ehlert, M. D. Burdick, R. M. Strieter, *J. Leukocyte Biol.* **2000**, *68*, 1 – 8.

[7] a) D. G. Duda, S. V. Kozin, N. D. Kirkpatrick, L. Xu, D. Fukumura, R. K. Jain, *Clin. Cancer Res.* **2011**, *17*, 2074 – 2080; b) C. V. Hinton, S. Avraham, H. K. Avraham, *Clin. Exp. Metastasis* **2010**, *27*, 97 – 105.

[8] E. De Clercq, *Nat. Rev. Drug Discovery* **2003**, *2*, 581 – 587.

[9] a) W. Zhan, Z. Liang, A. Zhu, S. Kurtkaya, H. Shim, J. P. Snyder, D. C. Liotta, *J. Med. Chem.* **2007**, *50*, 5655 – 5664; b) H. Tamamura, K. Hiramatsu, S. Kusano, S. Terakubo, N. Yamamoto, J. O. Trent, Z. Wang, S. C. Peiper, H. Nakashima, A. Otaka, *Org. Biomol. Chem.* **2003**, *1*, 3656 – 3662; c) H. Tamamura, K. Hiramatsu, M. Mizumoto, S. Ueda, S. Kusano, S. Terakubo, M. Akamatsu, N. Yamamoto, J. O. Trent, Z. Wang, *Org. Biomol. Chem.* **2003**, *1*, 3663 – 3669.

[10] a) A. Zhu, W. Zhan, Z. Liang, Y. Yoon, H. Yang, H. E. Grossniklaus, J. Xu, M. Rojas, M. Lockwood, J. P. Snyder, D. C. Liotta, H. Shim, *J. Med. Chem.* **2010**, *53*, 8556 – 8568; b) Z. Liang, W. Zhan, A. Zhu, Y. Yoon, S. Lin, M. Sasaki, J. M. Klapproth, H. Yang, H. E. Grossniklaus, J. Xu, M. Rojas, R. J. Voll, M. M. Goodman, R. F. Arrendale, J. Liu, C. C. Yun, J. P. Snyder, D. C. Liotta, H. Shim, *PLoS One* **2012**, *7*, e34038.

[11] a) H. Tamamura, A. Ojida, T. Ogawa, H. Tsutsumi, H. Masuno, H. Nakashima, N. Yamamoto, I. Hamachi, N. Fujii, *J. Med. Chem.* **2006**, *49*, 3412 – 3415; b) T. Narumi, H. Aikawa, T. Tanaka, C. Hashimoto, N. Ohashi, W. Nomura, T. Kobayakawa, H. Takano, Y. Hirota, T. Murakami, N. Yamamoto, H. Tamamura, *ChemMedChem* **2013**, *8*, 118 – 124; c) T. Tanaka, T. Narumi, T. Ozaki, A. Sohma, N. Ohashi, C. Hashimoto, K. Itotani, W. Nomura, T. Murakami, N. Yamamoto, H. Tamamura, *ChemMedChem* **2011**, *6*, 834 – 839.

[12] Z. Liang, T. Wu, H. Lou, X. Yu, R. S. Taichman, S. K. Lau, S. Nie, J. Umbreit, H. Shim, *Cancer Res.* **2004**, *64*, 4302 – 4308.

[13] B. Wu, E. Y. T. Chien, C. D. Mol, G. Fenalti, W. Liu, V. Katritch, R. Abagyan, A. Brooun, P. Wells, F. C. Bi, D. J. Hamel, P. Kuhn, T. M. Handel, V. Cherezov, R. C. Stevens, *Science* **2010**, *330*, 1066 – 1071.

[14] a) A. Brelot, N. Heveker, M. Montes, M. Alizon, *J. Biol. Chem.* **2000**, *275*, 23736 – 23744; b) W. T. Choi, S. M. Tian, C. Z. Dong, S. Kumar, D. X. Liu, N. Madani, J. An, J. G. Sodroski, Z. W. Huang, *J. Virol.* **2005**, *79*, 15398 – 15404.

[15] J. O. Trent, Z. X. Wang, J. L. Murray, W. H. Shao, H. Tamamura, N. Fujii, S. C. Peiper, *J. Biol. Chem.* **2003**, *278*, 47136 – 47144.

[16] a) A. M. Sun, D. C. Lankin, K. Hardcastle, J. P. Snyder, *Chem. Eur. J.* **2005**, *11*, 1579 – 1591; b) J. P. Snyder, N. S. Chandrakumar, H. Sato, D. C. Lankin, *J. Am. Chem. Soc.* **2000**, *122*, 544 – 545; c) D. C. Lankin, G. L. Grunewald, F. A. Romero, I. Y. Oren, J. P. Snyder, *Org. Lett.* **2002**, *4*, 3557 – 3560; d) D. C. Lankin, N. S. Chandrakumar, S. N. Rao, D. P. Spangler, J. P. Snyder, *J. Am. Chem. Soc.* **1993**, *115*, 3356 – 3357; e) H. H. Jensen, M. Bols, *Acc. Chem. Res.* **2006**, *39*, 259 – 265.

[17] H. Duewel, E. Daub, V. Robinson, J. F. Honek, *Biochemistry* **1997**, *36*, 3404 – 3416.

[18] a) J. Wess, *Mol. Pharmacol.* **2005**, *68*, 1506 – 1509; b) C. Trankle, A. Dittmann, U. Schulz, O. Weyand, S. Buller, K. Johren, E. Heller, N. J. M. Birdsall, U. Holzgrabe, J. Ellis, H. D. Holtje, K. Mohr, *Mol. Pharmacol.* **2005**, *68*, 1597 – 1610.

[19] G. E. DuBois, *Food Technology Magazine* (Institute of Food Technologists), September 2011, *vol. 65*, no. 9, p. 30; http://www.ift.org/past-issues/2011/september.aspx.

[20] ACD/Labs, Advanced Chemistry Development Inc.; http://www.acdlabs.com/home/.

[21] Glide, version 5.8, Schrödinger, LLC, New York, NY (USA), 2012; http://www.schrodinger.com.

[22] B. Jayaram, D. Sprous, D. L. Beveridge, *J. Phys. Chem. B* **1998**, *102*, 9571 – 9576.

[23] J. Dundas, Z. Ouyang, J. Tseng, A. Binkowski, Y. Turpaz, J. Liang, *Nucleic Acids Res.* **2006**, *34*, W116 – W118.

Received: December 18, 2012
Revised: January 3, 2013
Published online on March 6, 2013